JOURNAL OF STRUCTURAL CONTROL
J. Struct. Control 2002; **00**:1–6 *Prepared using* stcauth.cls *[Version: 2002/11/11 v1.00]*

Experimental study of the substructure isolation method for local health monitoring*

Jilin Hou[1,2,*], Łukasz Jankowski[2] and Jinping Ou[1,3]

[1] *School of Civil Engineering, Harbin Institute of Technology, Harbin 150090, P. R. of China*
[2] *Smart-Tech Centre, Institute of Fundamental Technological Research, Polish Academy of Sciences, Warsaw, Poland*
[3] *School of Civil and Hydraulic Engineering, Dalian University of Technology, Dalian 116024, P. R. of China*

SUMMARY

This paper extends and studies experimentally the substructure isolation method. Local health monitoring is significant for large and complex structures, since it costs less and can be easier implemented compared to global analysis. In contrast to other substructuring methods, in which the substructure is separated from the global structure, but coupled to it via the interface forces, the substructure isolation method isolates the substructure into an independent structure by placing virtual fixed supports on the interface. Model updating or damage identification can be then performed locally and precisely using the constructed responses of the isolated substructure and any of the existing methods aimed originally at global identification. This paper discusses and further extends the approach to improve its performance in real applications. A new type of virtual interface support (free support) is proposed for isolation. Relaxation of the original requirements concerning the type and placement of the isolating excitations is discussed. Previously, the method relied on the linearity of the global structure; here, only the substructure is required to be linear, the global structure besides the substructure can be nonlinear, yielding, changing or unknown. A damaged cantilever beam is used in the experimental study. Up to three modified global structures with the same substructure are used to test the robustness of the isolation with respect to unknown modifications and nonlinearities of the outside structure. Two typical global health monitoring methods are applied at the substructural level. A comparison with the results obtained from a generic substructure separation method is offered. Copyright © 2002 John Wiley & Sons, Ltd.

KEY WORDS: Structural health monitoring (SHM); Substructure isolation method; Substructural identification; Virtual distortion method (VDM); Local monitoring; Virtual supports

1. INTRODUCTION

In recent decades, Structure Health Monitoring (SHM) has become an important and widely researched field with a number of dedicated international journals and specialized international conferences. The research often focuses on practical applications in specialized structures, such as bridges, tall buildings,

*This is the **pre-peer reviewed version** of the following article: J. Hou, Ł. Jankowski, J. Ou, Experimental study of the substructure isolation method for local health monitoring, *Journal of Structural Control & Health Monitoring*, in press, doi: 10.1002/stc.443, which has been published in final form at `http://dx.doi.org/10.1002/stc.443`

*Correspondence to: hou.jilin@hotmail.com

dams, etc. In general, it is difficult and expensive to monitor such large and complex structures globally, especially as the boundary conditions, nonlinear components or the potential structural modifications can be hard to be determined or detected. Moreover, ill-conditioning, which is inherent in inverse problems of parametric structural identification, and large number of independent unknown parameters often undermine all efforts to achieve numerical convergence in large global identification problems. In fact, in most of cases only local substructures are crucial and need to be identified or monitored accurately. Therefore, methods which could extract local-only information from the locally measured response of the global structure would be very significant in practice.

At present, many methods have been proposed for damage localization. In the static or quasi-static cases, the analysis is usually based on global or local structural flexibilities. Park et al. partition in [1] decompose the global flexibility matrix into substructural flexibilities, which can be also obtained based on local measurements, and propose localized damage indicators based on their relative changes. In [2], an invariance property of the transmission zeros of the substructural frequency response functions is used to localize the damage. Bernal et al. [3, 4] consider the matrix which represent the change of the global flexibility and define Damage Locating Vectors (DLVs) to be the basis of its null space; all traceable damaged elements have to belong to the corresponding zero stress regions. Gao and Spencer [5] develop further the method of DLVs to include the ambient vibration case. However, as the structural flexibility is a static characteristics of the structure, it may contain less information than the dynamic response: some damages types can be evident in a dynamic analysis but masked in a static-only analysis.

Substructuring techniques, which are used in dynamic analysis, are usually model-based and focus on separation of the analyzed substructure from the global structure by partitioning the global equation of motion. That is, the substructure is treated as having free boundary conditions on its interface with the global structure, and the influence on the global structure is represented by the generalized interface forces. As these forces are unknown, they have to be identified or estimated along with the unknown physical parameters of the substructure (mass, stiffness, damping). In the context of structural identification, the substructural approach has been probably first proposed by Koh et al. in [6] and called a substructural identification (SSI) or a divide-and-conquer strategy. A method based on the extended Kalman filter with weighted global iteration is formulated there for substructures with and without overlapping members; in [7], it is developed into a progressive structural identification approach, which is aimed at the identification of global structure through identification of progressively growing substructures. The extended Kalman filter is used also by Oreta and Tanabe [8] for local identification of member properties in framed structures. In [9], Yun and Lee locally estimate unknown parameters related to damages using an ARMAX model of the substructure and a sequential prediction error method. Complete measurement of the substructure is necessary, including the interior excitations and the response in all degrees of freedom (DOFs). Tee et al. [10] apply the substructural strategy to structural health monitoring, and based on the eigensystem realization algorithm and the observer/Kalman filter, propose two methods aimed at first- and second-order model identification and damage assessment at the substructural level. In [11], they are combined with a model condensation approach in order to reduce the number of necessary measurements. In all these and similar methods, complete measurement of interface response is necessary: the measured response is then treated as an input to the substructure. In [12], Koh et al. use local frequency response functions to identify interface forces simultaneously with the unknown physical parameters of the substructure. Different sets of internal response measurements are used to the obtain estimates of interface forces, and the identification procedure amounts to minimization of the discrepancy between the estimates. The interface measurements are not necessary. Yang and Huang propose in [13] a sequential nonlinear least-square method to estimate unknown excitations, physical parameters of the substructure as well as the interface forces between the substructure and the global structure. The method only requires only a limited number of acceleration responses, and it can trace a damage changing with time. Yun et al. [14] propose a method for local monitoring of stiffness modifications using a neural network, where the input vector consists of natural frequencies and locally measured incomplete global mode shapes. Complete measurement of the substructure is not required, but a numerical model of the unmodified global structure is necessary.

All these and similar methods can be collectively called *substructure separation* methods, since the substructure is not fully isolated from the global structure: though separated, they are coupled to each other via unknown interface forces. The identification procedure has to account for these forces, which often considerably increases the numerical costs. As a result, the proposed identification methods, although effective, are non-standard and have to be specifically tailored to be used on the substructural level. Standard and widely-researched model updating or health monitoring methods cannot be directly applied to the separated substructure. To overcome this drawback, Hou et al. have proposed in [15] the *substructure isolation* method. The core idea of the method is different: instead of building the equation of motion of the substructure and accounting for the interface forces, the method eliminates the outside influences of the global structure from the measured responses of the substructure. The substructure behaves then as fully isolated and responds to internal excitations only, so that its constructed response can be used with any of the standard model updating or health monitoring methods. The isolation process is equivalent to placing virtual fixed supports on the interface, which are implemented by sensors (accelerometers or others) placed in all DOFs of the interface; the number and placement of the internal sensors depend entirely on the follow-on identification/monitoring method. Response of the isolated substructure is directly constructed using measured responses of the substructure, so that no parametric numerical model is required for the isolation.

This paper discusses and further extends the substructure isolation method to improve its performance in real applications. Besides the virtual fixed supports, a new type of virtual interface support (free support) is proposed for isolation. Relaxation of the original requirements concerning the type and placement of the isolating excitations is discussed. Previously, the method relied on the assumptions of linearity of the global structure; here, only the substructure is required to be linear, the global structure besides the substructure can be nonlinear, yielding, changing or simply unknown. In the derivations, a formal continuous-time formulation is used, which is stricter and more concise than the discrete-time setting used before. Moreover, this paper substantiates the method with an experimental study. A damaged cantilever beam is used to validate the isolation methodology and to perform local damage identification. Up to three different global structures with the same substructure (the original beam with an optional "sponge support" or a mass) are used to test the robustness of the isolation with respect to unknown modifications and nonlinearities of the outside structure. Two typical global health monitoring methods are applied at the substructural level, so that the damage is identified based on comparison of either time-domain responses of the substructure or its modal characteristics. In all cases the substructure is successfully isolated and the damages are locally identified. A comparison with the results obtained from a custom generic substructure separation method is also offered.

The paper is structured as follows: the next section provides a brief review of the original formulation of the substructure isolation method. The substructure is isolated with virtual fixed supports, the global structure is assumed to be linear, and the constraining excitations are impulsive and applied on the interface. These limitations can be relaxed or dropped, which is described in the third section. The fourth section discusses practical application of the method (discretization, measurements and excitations, damage identification). The last section reports on the experimental study.

Prepared using stcauth.cls

2. SUBSTRUCTURE ISOLATION METHOD

This section reviews the substructure isolation method. A continuous-time formulation is used, which seems to be more concise than the original discrete-time setting [15]. Linearity of the global structure and impulsive interface excitations are assumed for simplicity. These restrictions are inessential and can be significantly relaxed, as described in the next section. The substructure is isolated from the global structure by placing virtual fixed supports in all degrees of freedom (DOFs) of the interface between them. In agreement with the general approach of the virtual distortion method (VDM) [16, 17, 18], the response of such an isolated substructure can be expressed as a sum of the responses of the global structure to

1. the same load (the corresponding responses are directly measured) and to
2. certain generalized virtual forces that act in all DOFs of the interface in order to model the fixed supports (the corresponding responses are constructed using the measured responses).

A DOF is properly fixed-supported, if its response vanish. The virtual forces can be thus computed using the condition that the responses in all interface DOFs vanish. Thereupon, the response of any linear sensor placed inside the isolated substructure can be constructed by using the same principle of superposition of the measured response of the global structure and the responses to the computed virtual forces.

Let the global structure be externally excited by loads $\mathbf{P}(t)$, which can include loads $\mathbf{P}_{\mathrm{s}}(t)$ applied inside the concerned substructure and loads $\mathbf{P}_{\mathrm{e}}(t)$ applied on the substructure interface or outside it. Denote the corresponding response (displacement, velocity or acceleration) in the ith DOF of the interface by $a_i^{\mathrm{M}}(t)$, and the response (any kind of linear dynamic response) of the αth sensor placed inside the substructure by $u_\alpha^{\mathrm{M}}(t)$. Assume zero initial conditions of the global structure. In order to isolate the substructure from the global structure, starting from time $t = 0$, virtual fixed supports are added in all DOFs of the interface of the substructure in the form of the virtual forces $f_i^0(t)$, which are intended to model the support reaction forces. As the global structure is assumed to be linear, the responses of the structure can be expressed as the following sums of the measured original responses and the cumulative effects of the virtual forces:

$$a_i(t) = a_i^{\mathrm{M}}(t) + \sum_j \int_0^t B_{ij}^0(t-\tau) f_j^0(\tau)\, d\tau, \tag{1a}$$

$$u_\alpha(t) = u_\alpha^{\mathrm{M}}(t) + \sum_j \int_0^t D_{\alpha j}^0(t-\tau) f_j^0(\tau)\, d\tau, \tag{1b}$$

where $B_{ij}^0(t)$ and $D_{\alpha j}^0(t)$ denote the impulse-responses of the global structure that relate an impulse load in the jth interface DOF to the responses in the ith interface DOF and of the αth inner sensor, respectively. If the responses are accelerations, the impulse-responses can contain an impulsive component at $t = 0$. Equations 1, collected for all interface DOFs and all inner sensors, can be stated in the form of the following operator equations:

$$\mathbf{a} = \mathbf{a}^{\mathrm{M}} + \boldsymbol{\mathcal{B}}^0 \mathbf{f}^0, \tag{2a}$$

$$\mathbf{u} = \mathbf{u}^{\mathrm{M}} + \boldsymbol{\mathcal{D}}^0 \mathbf{f}^0, \tag{2b}$$

where $\boldsymbol{\mathcal{B}}^0$ and $\boldsymbol{\mathcal{D}}^0$ are the respective matrix operators. Since the interface DOFs in the isolated substructure are fixed-supported, the responses $\mathbf{a}(t)$ vanish in Eq. (2a) and the reaction forces of the virtual fixed supports can be found by solving the following operator equation:

$$\boldsymbol{\mathcal{B}}^0\mathbf{f}^0 = -\mathbf{a}^{\mathrm{M}}, \tag{3}$$

which is usually ill-conditioned and can be solved only in the regularized sense [19]. The solution can be substituted in Eq. (2b) to obtain the responses of the inner sensors in the isolated substructure:

$$\mathbf{u} = \mathbf{u}^{\mathrm{M}} - \boldsymbol{\mathcal{D}}^0\left[\boldsymbol{\mathcal{B}}^0\right]^{\star}\mathbf{a}^{\mathrm{M}}, \tag{4}$$

where the superscript $\star$ denotes the (regularized) inverse of a matrix operator.

In this way, by Eq. (3) and the assumption of zero initial conditions, the response of the substructure interface is zeroed. This is achieved by adding virtual fixed supports, properly modelled by their reaction forces $\mathbf{f}^0(t)$. As a result, the substructure is isolated from the rest of the global structure, and it behaves as a new and independent structure that is called the *isolated substructure*. Since its interface is constrained, the inner sensors respond by Eq. (4) only to the inner loads $\mathbf{P}_{\mathrm{s}}(t)$ and are separated from the loads $\mathbf{P}_{\mathrm{e}}(t)$ that occur on the interface or outside it, including the loads used to generate the impulse-responses $B^0_{ij}(t)$ and $D^0_{\alpha j}(t)$. As evident in Eq. (4), the sensors placed on the boundary contribute to the isolation via their measurements $\mathbf{a}^{\mathrm{M}}(t)$. From a certain point of view, these sensors can be said to play the role of the virtual fixed supports.

3. PRACTICAL EXTENSIONS OF THE ISOLATION METHOD

The response of the isolated substructure is constructed using the structural impulse-responses $B^0_{ij}(t)$ and $D^0_{\alpha j}(t)$, which will be called the *constraining responses*, as they are used to constrain the response of the interface. Similarly, $a^{\mathrm{M}}_j(t)$ and $u^{\mathrm{M}}_\alpha(t)$ will be called the *basic responses*. In practice, these responses must be measured experimentally prior to the isolation. Let the corresponding excitations be respectively called the *constraining excitations* and the *basic excitations*. The substructure isolation method, as described in Section 2, relies on the following four assumptions:

1. virtual supports are fixed,
2. constraining excitations are applied in the DOFs of the substructure interface,
3. constraining excitations are impulsive,
4. global structure is linear.

In practice, these assumptions are hard to be satisfied and limit the application possibilities of the method. In this section, they are significantly relaxed, so that virtual free supports can be used for isolation besides the fixed supports, and the constraining excitations can be of any type and placed also outside the substructure interface. Moreover, the method turns out to be applicable also in the cases when the global structure, apart from the substructure, reveals unknown nonlinear/nonelastic behavior or is changing, or even unknown. The extensions introduced below are intended to make the substructure isolation method more feasible and easier implementable in real applications.

3.1. Virtual free supports

Sometimes it can be hard to obtain the measurements in all DOFs of the substructure interface, as required for the fixed support isolation. For example, consider a structure consisting of two frames connected with a single beam, see Figure 1 (left). Let the right-hand part of the structure be the

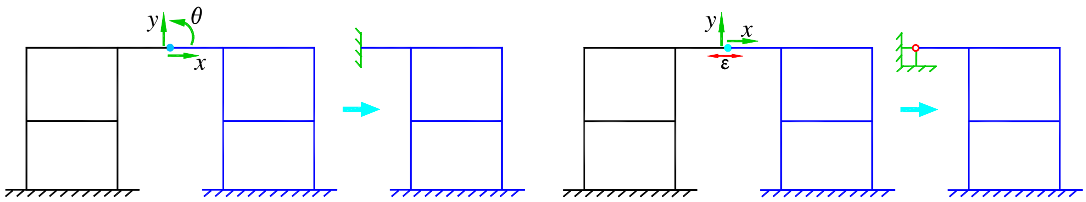

Figure 1. Isolation of a frame substructure: (*left*) three virtual fixed supports in the interface DOFs; (*right*) two fixed and one free virtual support in the interface DOFs (a single pinned support in the interface node)

concerned substructure. There are three DOFs on the substructure interface, that is the horizontal displacement x, the vertical displacement y and the rotational displacement θ. For the fixed support isolation, the responses $a_x^{\mathrm{M}}(t)$, $a_y^{\mathrm{M}}(t)$ and $a_\theta^{\mathrm{M}}(t)$ in all these three DOFs need to be measured. The substructure can be then isolated by the following conditions, which are together equivalent to Eq. (3):

$$a_x(t) = 0 \qquad a_y(t) = 0 \qquad a_\theta(t) = 0. \tag{5}$$

In practice, it is usually more convenient to measure the strain ε than the rotation θ. Moreover, the measured strain can be related to the internal bending moment, which at the cross-section is proportional to the difference between the strains measured on the opposite faces of the beam, $a_\varepsilon^{\mathrm{M}} = a_{\varepsilon_1}^{\mathrm{M}} - a_{\varepsilon_2}^{\mathrm{M}}$; if the axial distortion is negligible, as in the experiment described in this paper, a single strain measurement is sufficient. Thus, instead of the rotational displacement, it is possible to require the internal bending moment to vanish on the interface of the isolated substructure, which is formally expressed by

$$a_x(t) = 0 \qquad a_y(t) = 0 \qquad a_\varepsilon(t) = 0, \tag{6}$$

which are the conditions for a virtual pinned support in the interface node, as illustrated in Figure 1 (right). Such a support consists of two fixed virtual supports, which constrain the horizontal and the vertical DOFs, and a single free virtual support, which constrains the internal bending moment at the cross-section and thus enables free rotation.

Because of their practicality in real applications, free virtual supports seem to be more advantageous and feasible for rotational interface DOFs than fixed virtual supports.

3.2. Placement of the constraining excitations

In Section 2, the response of the isolated substructure is derived under the assumption that the constraining excitations (unit impulses) are applied on the interface of the substructure. This requirement is not always practical: sometimes there can be already a lot of sensors on the interface or it can be inaccessible for precise excitations, especially for moment excitations. In many cases, it can be easier and more accurate to use force excitations instead, and to place them outside the interface.

The substructure isolation method allows the placement requirement to be significantly relaxed, so that the constraining excitations can be placed in principle anywhere on the interface or outside it. Even if placed outside, they modify the internal interface forces, and so they still can be used to constrain the response of the interface and implement the supports. Let the virtual forces $f_\beta^0(t)$ be placed in any DOF of the interface or outside it and index all these DOFs by β. Since the global structure is (still) assumed to be linear, there exists a linear operator $\boldsymbol{\mathcal{F}}$ that transforms the vector of all virtual forces $\mathbf{f}^0$

into the vector $\mathbf{p}$ of the total interface forces, which act on the substructure and include the internal forces as well as, in case they are applied on the interface, the virtual forces,

$$\mathbf{p} = \boldsymbol{\mathcal{F}}\mathbf{f}^0. \tag{7}$$

As the vector $\mathbf{p}$ denotes the total interface forces, the substructure responds in the same way to $\mathbf{f}^0$ and to $\mathbf{p}$. Therefore, similarly as in Eq. (2), the response of the substructure to the loads $\mathbf{P}(t)$ and $\mathbf{f}^0$ can be then expressed as

$$\mathbf{a} = \mathbf{a}^{\mathrm{M}} + \boldsymbol{\mathcal{B}}^{\mathrm{B}}\mathbf{p} = \mathbf{a}^{\mathrm{M}} + \boldsymbol{\mathcal{B}}^{\mathrm{B}}\boldsymbol{\mathcal{F}}\mathbf{f}^0, \tag{8a}$$

$$\mathbf{u} = \mathbf{u}^{\mathrm{M}} + \boldsymbol{\mathcal{D}}^{\mathrm{B}}\mathbf{p} = \mathbf{u}^{\mathrm{M}} + \boldsymbol{\mathcal{D}}^{\mathrm{B}}\boldsymbol{\mathcal{F}}\mathbf{f}^0, \tag{8b}$$

where the linear matrix operators $\boldsymbol{\mathcal{B}}^{\mathrm{B}}$ and $\boldsymbol{\mathcal{D}}^{\mathrm{B}}$ relate the interface forces to the corresponding responses of the substructure with all free boundary conditions. The forms of Eqs. (2) and Eqs. (8) are the same and thus the response of the isolated substructure can be still expressed as in Eq. (4),

$$\mathbf{u} = \mathbf{u}^{\mathrm{M}} - \boldsymbol{\mathcal{D}}^0 \left[\boldsymbol{\mathcal{B}}^0\right]^{\star} \mathbf{a}^{\mathrm{M}}, \tag{9}$$

where the matrix operators

$$\boldsymbol{\mathcal{B}}^0 = \boldsymbol{\mathcal{B}}^{\mathrm{B}}\boldsymbol{\mathcal{F}} \qquad\qquad \boldsymbol{\mathcal{D}}^0 = \boldsymbol{\mathcal{D}}^{\mathrm{B}}\boldsymbol{\mathcal{F}} \tag{10}$$

correspond to the measured constraining responses and are thus known. Therefore, the response of the interface can be zeroed also when the constraining excitations are applied outside the substructure, provided the corresponding version of Eq. (3) is solvable. However, as the placement of the constraining excitations can affect also its conditioning and so the accuracy of the isolation, it should be chosen with care: few practical hints are provided in Section 4.2.

Notice that the virtual forces $f^0_\beta(t)$, if placed outside the interface, cease to be the reaction forces of the virtual supports. Instead, they are rather used to modify the total interface forces, so that they play the role of the reaction forces of the virtual interface supports that isolate the substructure. Notice also that outside the interface, as demonstrated in the experiments described below, it is possible to use force excitations instead of moment excitations, which is often more feasible in practice.

3.3. Non-impulsive constraining excitations

In practice, the constraining responses $B^0_{i\beta}(t)$ and $D^0_{\alpha\beta}(t)$ are measured as responses to the experimentally applied constraining excitations, which are unit impulses. However, the ideal impulse is hard to apply and so the exact impulse-responses may not be easy to obtain. Nevertheless, it is possible to measure the responses $B_{i\beta}(t)$ and $D_{\alpha\beta}(t)$ to any non-impulsive excitations $q_\beta(t)$ that are technically feasible and easy to apply. These responses can be also used as the constraining responses, provided the virtual forces $f^0_\beta(t)$ can be expressed in the form of the following convolution:

$$f^0_\beta(t) = \left(q_\beta * f_\beta\right)(t) = \int_0^t q_\beta(t-\tau) f_\beta(\tau)\, d\tau, \tag{11}$$

where $f_\beta(t)$ are certain unknown functions and $q_\beta(t)$ are the actually applied non-impulsive excitations, which have to satisfy $q_\beta\,(t) = 0$ for $t < 0$. Equation 11, collected for all β, takes in the operator notation the following form:

$$\mathbf{f}^0 = \boldsymbol{\mathcal{Q}}\mathbf{f}, \tag{12}$$

where $\mathcal{Q}$ is the corresponding diagonal matrix convolution operator. The reaction forces $\mathbf{p}(t)$ of the virtual supports are then linearly dependent on the vector $\mathbf{f}(t)$:

$$\mathbf{p} = \mathcal{F}\mathcal{Q}\mathbf{f}. \tag{13}$$

Similarly as in Eqs. (8), the response of the substructure can be then expressed as

$$\mathbf{a} = \mathbf{a}^{\mathrm{M}} + \mathcal{B}^{\mathrm{B}}\mathcal{F}\mathcal{Q}\mathbf{f} = \mathbf{a}^{\mathrm{M}} + \mathcal{B}\mathbf{f}, \tag{14a}$$

$$\mathbf{u} = \mathbf{u}^{\mathrm{M}} + \mathcal{D}^{\mathrm{B}}\mathcal{F}\mathcal{Q}\mathbf{f} = \mathbf{u}^{\mathrm{M}} + \mathcal{D}\mathbf{f}. \tag{14b}$$

The matrix operators $\mathcal{B}$ and $\mathcal{D}$ can be shown to be of the following form:

$$(\mathcal{B}\mathbf{f})(t) = (\mathbf{B} * \mathbf{f})(t) = \int_0^t \mathbf{B}(t-\tau)\mathbf{f}(\tau)\, d\tau, \tag{15a}$$

$$(\mathcal{D}\mathbf{f})(t) = (\mathbf{D} * \mathbf{f})(t) = \int_0^t \mathbf{D}(t-\tau)\mathbf{f}(\tau)\, d\tau, \tag{15b}$$

where the matrices $\mathbf{B}(t) = [B_{i\beta}(t)]$ and $\mathbf{D}(t) = [D_{\alpha\beta}(t)]$ collect the experimentally measured constraining responses to the non-impulsive excitations $q_\beta(t)$. Equations 14 yield a formula similar to Eqs. (4) and (9),

$$\mathbf{u} = \mathbf{u}^{\mathrm{M}} - \mathcal{D}\mathcal{B}^{\star}\mathbf{a}^{\mathrm{M}}, \tag{16}$$

which can be used to compute the response of the isolated substructure using non-impulsive constraining excitations. Notice that these excitations do not occur in Eq. (16), so that they even need not be measured.

3.4. Nonlinearity of the outside structure

The substructure isolation method and its extensions, as described in the above sections, are derived based on the assumption of the linearity of the global structure. This assumption may not be easy to verify and may not always hold due to various common reasons such as joint imperfections, unknown boundary conditions, dry friction, etc. Nevertheless, the method remains valid as long as the substructure itself is linear. Such a substructure can be isolated irrespective of the properties of the outside structure, which can be nonlinear, nonelastic or changing during the measurements, or simply unknown. Basically, a similar argument is used as in Section 3.2: virtual supports for a linear substructure are modeled via virtual modifications of the total interface forces. In this way, the isolation process is focused on the substructure, which is effectively treated as having all boundary conditions free and thus linear.

Denote by $\mathbf{p}_\beta(t)$ the (unknown) vector of the total interface forces that act on the substructure in the effect of a given constraining excitation $q_\beta(t)$, which may be non-impulsive and placed outside the interface. The forces $\mathbf{p}_\beta(t)$ include all the internal forces and also the constraining excitation $q_\beta(t)$ in case it is placed in an interface DOF, so that the response of the substructure to $q_\beta(t)$ is the same as the response to $\mathbf{p}_\beta(t)$ of the same substructure with all free boundary conditions. For isolation, the virtual supports are placed in all interface DOFs of the substructure. As the global structure may be nonlinear, the reaction forces $\mathbf{p}(t)$ of the virtual supports cannot be modeled in a linear way as in Eq. (13). However, the response of the substructure with all free boundary conditions is linearly dependent on its interface forces, so that the reaction forces $\mathbf{p}(t)$ can be modeled using a linear convolution of the total interface forces $\mathbf{p}_\beta(t)$ instead of the constraining excitations,

$$\mathbf{p}(t) = \sum_\beta (\mathbf{p}_\beta * f_\beta)(t) = \sum_\beta \int_0^t \mathbf{p}_\beta(t-\tau) f_\beta(\tau)\, d\tau, \tag{17}$$

where $f_\beta(t)$ are certain unknown functions. In the operator notation, Eq. (17) takes the following form:

$$\mathbf{p} = \boldsymbol{\mathcal{P}}\mathbf{f}, \tag{18}$$

where $\boldsymbol{\mathcal{P}}$ is the corresponding (unknown) linear matrix convolution operator. Similarly as in Eqs. (8) and (14), the response of the substructure can be then expressed in the form of the following linear operator equations:

$$\mathbf{a} = \mathbf{a}^{\mathrm{M}} + \boldsymbol{\mathcal{B}}^{\mathrm{B}}\boldsymbol{\mathcal{P}}\mathbf{f} = \mathbf{a}^{\mathrm{M}} + \boldsymbol{\mathcal{B}}\mathbf{f}, \tag{19a}$$

$$\mathbf{u} = \mathbf{u}^{\mathrm{M}} + \boldsymbol{\mathcal{D}}^{\mathrm{B}}\boldsymbol{\mathcal{P}}\mathbf{f} = \mathbf{u}^{\mathrm{M}} + \boldsymbol{\mathcal{D}}\mathbf{f}, \tag{19b}$$

where the matrix operators $\boldsymbol{\mathcal{B}}$ and $\boldsymbol{\mathcal{D}}$ can be shown to be of the same form as in Eqs. (15) and thus known. Equations 19 have the same form as Eqs. (14), and hence the response of the isolated substructure can be expressed as in Eq. (16).

Notice that the functions $f_\beta(t)$ in Eqs. (17) and (19) cease not only to be the virtual reaction forces of the modeled supports but also to be any virtual forces at all. They are an artificial construct, which is used to represent such virtual modifications of the total interface forces that they play the role of the reaction forces of the virtual supports.

4. APPLICATION OF THE METHOD

4.1. *Discrete responses*

For theoretical clarity, all the responses have been so far assumed to be continuous. However, in a real application only discrete data can be measured. In practice, all the responses are thus available in the form of vectors that are sampled in discrete time points every Δt. Therefore, the key formula Eq. (16) has to be accordingly discretized to the following form:

$$\tilde{\mathbf{u}} = \tilde{\mathbf{u}}^{\mathrm{M}} - \tilde{\mathbf{D}}\tilde{\mathbf{B}}^{\star}\tilde{\mathbf{a}}^{\mathrm{M}}, \tag{20}$$

where, with proper ordering of the data, the matrices $\tilde{\mathbf{B}}$ and $\tilde{\mathbf{D}}$ take the forms of large block matrices with Toeplitz blocks. As an example, Figure 2 illustrates the structure of a matrix $\tilde{\mathbf{B}}$ obtained in the experimental study described below. Matrices of this kind are usually extremely ill-conditioned [20], and hence the superscript $\star$ denotes in Eq. (20) the regularized pseudoinverse that can be computed e.g. via the truncated singular value decomposition (TSVD). However, the term $\tilde{\mathbf{B}}^{\star}\tilde{\mathbf{a}}^{\mathrm{M}}$ denotes a regularized solution of the following discretized version of Eq. (3),

$$\tilde{\mathbf{B}}\tilde{\mathbf{f}} = -\tilde{\mathbf{a}}^{\mathrm{M}}, \tag{21}$$

and it can be found using any of the direct or iterative methods.

4.2. *Measurements and excitations*

Equation 20 shows that the following measurements of the global structure are necessary for isolation:

- The discrete *constraining responses* $\tilde{B}_{i\beta}(t)$ and $\tilde{D}_{\alpha\beta}(t)$, which are the responses of the interface and the inner sensors to the constraining excitations $q_\beta(t)$.
- The discrete *basic responses* $\tilde{a}_i^{\mathrm{M}}(t)$ and $\tilde{u}_\alpha^{\mathrm{M}}(t)$ of the interface and the inner sensors to the basic excitation $\mathbf{P}(t)$, which includes the deliberately applied inner excitations $\mathbf{P}_{\mathrm{s}}(t)$ and possibly, the outside and interface excitations $\mathbf{P}_{\mathrm{e}}(t)$.

Prepared using stcauth.cls

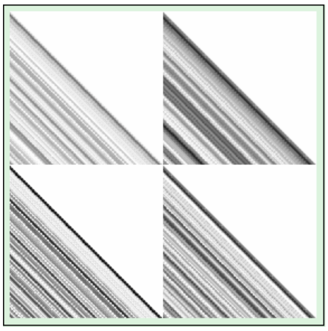

Figure 2. Structure of a constraining matrix $\tilde{\mathbf{B}}$ obtained in the experiment

The inner basic excitation $\mathbf{P}_{\mathrm{s}}(t)$ is applied inside the inner substructure to gather dynamic information about it for local identification or health monitoring. The outside and interface excitations $\mathbf{P}_{\mathrm{e}}(t)$ can be unknown. The constraining excitations $q_\beta(t)$ are applied on the interface or outside of it in order to yield the constraining responses, which are then used to construct the response of the isolated substructure. Basically, the constraining excitations can be of any type and even need not be measured. However, their character and placement influence the conditioning of Eq. (21), which is usually significantly ill-conditioned, but still solvable in the regularized sense. Its conditioning can be improved, if the constraining responses provide full dynamic information about the interface of the substructure. The following practical hints can be considered:

1. In order to ensure a high signal-to-noise ratio, it is better to place the constraining excitations near the interface rather than far away from it.
2. It is better to apply the constraining excitations in different points and in various directions. In this way, there are more chances that the constraining responses are independent.
3. The constraining excitations should not be very soft or too hard. A soft excitation may excite only low frequencies, while a hard excitation may result in only high-frequency response. In both cases, information at some frequency range is lost, which can worsen the conditioning of the system matrix or even make it rank-deficient.

4.3. Substructure identification

Using Eq. (20), the response of the isolated substructure to the inner basic excitation $\mathbf{P}_{\mathrm{s}}(t)$ can be constructed from the measurements. All standard and well-investigated methods of identification and monitoring can be thus applied locally, so that modeling of the global structure is avoided, which can significantly decrease the monitoring costs in real applications. Here, according to the character of the basic excitation, the substructure is identified in time domain and in mode domain.

4.3.1. Identification in time domain Provided $\mathbf{P}_{\mathrm{s}}(t)$ is known, local damage of the substructure can be identified via a time-domain comparison of the constructed response $\tilde{\mathbf{u}}$ with the response $\hat{\mathbf{u}}$ that is computed using a numerical model of isolated substructure. Let $\boldsymbol{\mu}$ be the vector of unknown structural parameters that represent the damage. It can be treated as the optimization variable, and the damage can be identified by a minimization of the following objective function:

$$\eta_1(\boldsymbol{\mu}) = \frac{\|\tilde{\mathbf{u}} - \hat{\mathbf{u}}(\boldsymbol{\mu})\|^2}{\|\tilde{\mathbf{u}}\|^2}, \tag{22}$$

which is the normalized least-square distance between the constructed response $\tilde{\mathbf{u}}$ and the computed response $\hat{\mathbf{u}}(\boldsymbol{\mu})$ of the isolated substructure.

4.3.2. Identification in mode domain Let $\mathbf{P}_\mathrm{s}(t)$ be a short-time quasi-impact load that need not be measured. Then, after the impact load disappears, the constructed response is the free response of the isolated substructure, because there is no excitation applied to the inner substructure. Using the constructed free response, the modes of the isolated substructure, including its natural frequencies $\tilde{\omega}_i$ and mode shapes $\tilde{\boldsymbol{\varphi}}_i$, can be identified by the Eigensystem Realization Algorithm (ERA) [24]. A local damage of the substructure can be then identified via a mode-domain comparison of the identified modes with the modes that are computed using a numerical model of isolated substructure, that is the damage vector $\boldsymbol{\mu}$ can be identified by a minimization of the following objective function:

$$\eta_2(\boldsymbol{\mu}) = \sum_i \left| \frac{\tilde{\omega}_i - \hat{\omega}_i(\boldsymbol{\mu})}{\tilde{\omega}_i} \right|^2 + \sum_i k_i \left| 1 - \mathrm{MAC}\left(\tilde{\boldsymbol{\varphi}}_i, \hat{\boldsymbol{\varphi}}_i(\boldsymbol{\mu})\right) \right|^2, \tag{23}$$

where $\hat{\omega}_i(\boldsymbol{\mu})$ and $\hat{\boldsymbol{\varphi}}_i(\boldsymbol{\mu})$ are respectively the ith natural frequency and mode shape of the numerical model of the isolated substructure, and k_i is a weighting factor of the ith mode shape error that is computed using the Modal Assurance Criterion (MAC).

5. EXPERIMENTAL STUDY

A damaged aluminum cantilever beam is used in the experimental study of the substructure isolation method and local damage identification. A comparison with the results obtained from a generic custom substructure separation method is included.

5.1. Experimental setup

The experimental setup is shown in Figure 3. The specimen, an aluminum cantilever beam, has the length of 136.15 cm and a rectangular cross-section of 2.7 cm × 0.31 cm. The fixed end is clamped to a stable frame, which is seen in blue on the left-hand side of Figure 3. Young's modulus of the beam is 70 GPa, and the density is 2700 kg/m^3. The beam is slender, thus the axial distortions are neglected, but the gravity is considered. The upper part of the beam (of length 79.4 cm) is the substructure to be identified. It is damaged by cutting even notches near the fixed end on the length of 10.2 cm, which decreases the stiffness of the damaged segment to 42% of its original stiffness and leaves the mass nearly unchanged, see Figure 4.

In the inner of the substructure, at the location denoted by P1, basic excitations of two kinds are applied separately to be used with different identification methods:

1. a windowed sine pulse $\sin(60\pi t)$, denoted by f_1, see Figure 5, is applied using an Amplified Piezo Actuator (APA) (Figure 3) for identification in time domain using the substructure isolation and the substructure separation methods. The APA is fixed to the inner substructure in such a way that it can be assumed to apply a pure moment load.

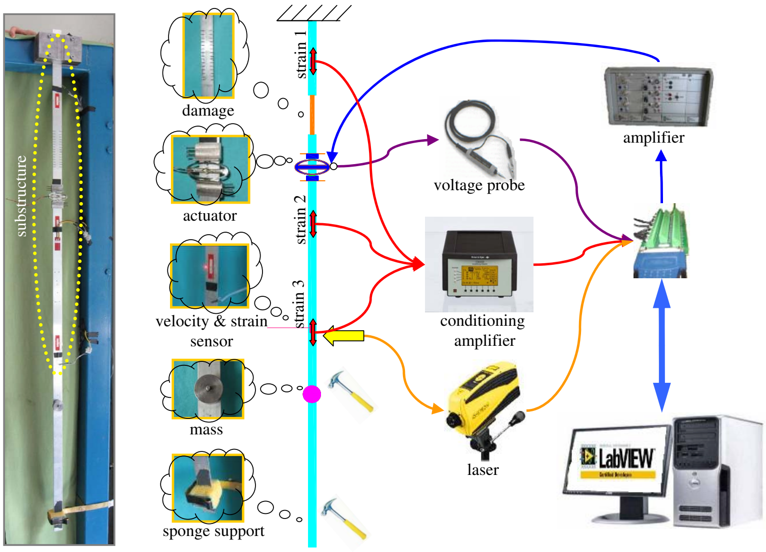

Figure 3. Experimental setup

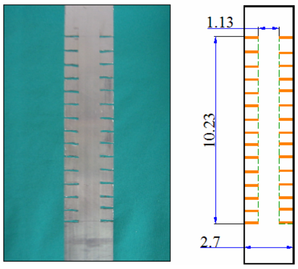

Figure 4. The damage (stiffness decreased, mass unchanged)

2. a simple hammer impact is taken as the basic excitation for identification in mode domain using the proposed isolation method.

Three piezoelectric patches are glued to the beam to measure the structural strain, and the transverse interface velocity is measured using a laser vibrometer, see Figure 3. Responses of these sensors are denoted respectively by Y1, Y2, Y3 and Y4, see Table I. The measurement data, including the excitation f_1, is acquired and stored on a PC via the acquisition system LabVIEW. Two amplifiers are used to amplify the signals from the strain sensors (Y1, Y2 and Y3) and the excitation signal f_1. To reduce the measurement noise, each excitation is repeated 4 to 5 times and the averaged responses are used for identification. The sampling frequency is chosen to be 10 kHz in order to guarantee that the sampled data contain all the necessary dynamic information about the substructure. The considered sampling time is 0.4 s, so that there are 4000 time steps.

In addition, three different global structures with the same substructure are used in order to verify the robustness of the isolation with respect to unknown modifications or nonlinearities of the outside

Prepared using stcauth.cls

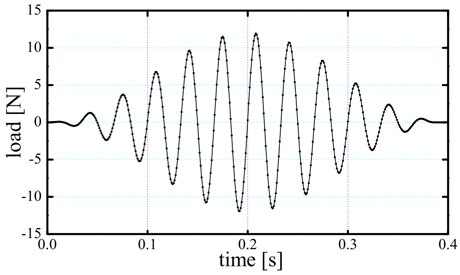

Figure 5. The basic excitation: a windowed sine pulse ($\sin 60\pi t$) exited at P1 by the piezo-actuator

Table I. Sensors and responses

symbol	measurand	position
Y1	strain 1	upper inner substructure
Y2	strain 2	lower inner substructure
Y3	strain 3	interface
Y4	transverse velocity	interface

Table II. The three global structures with the same substructure

symbol	outside structure
B1	original beam
B2	original beam with an additional unknown mass
B3	original beam with a “sponge support”

structure. Based on the same beam, the outside structure is modified by fixing an unknown additional mass or by mounting a “sponge support” in place of the free end, see Table II and Figure 3. The sponge support can increase the structural damping and may have nonlinear characteristics. Under the excitation f_1, the corresponding basic responses of the four sensors are measured in all three global structures, see Figure 6. The responses of the three structures differ significantly except for Y2 (“strain 2”), which confirms that the three structures are different. The sensor “strain 2” is located close to the actuator, and it responds mainly to the excitation.

In the following sections, both the generic substructure separation method and the substructure isolation method are tested and compared using the same measured data:

1. *Separation with interface forces.* Using the generic approach, the substructure is separated from the global structure with free boundary, while the unknown interface forces are explored. The damages of the substructure and the interface forces are identified simultaneously.
2. *Isolation with virtual supports.* The response of the isolated substructure is constructed using the substructure isolation method. The local damage is then identified in time domain and in mode domain according to the type of the basic excitation.

Prepared using stcauth.cls

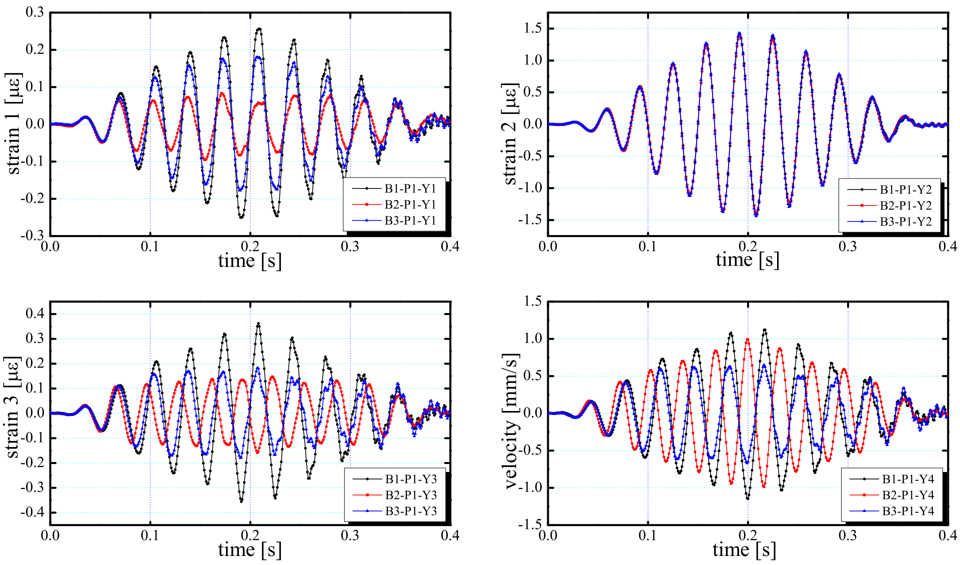

Figure 6. Measured basic responses of the three considered global structures: (*upper left*) strain Y1; (*upper right*) strain Y2; (*bottom left*) strain Y3; (*bottom right*) velocity Y4

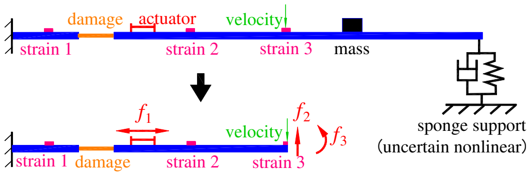

Figure 7. Substructure is separated with a free boundary and interface forces (separated substructure)

5.2. *Separation with interface forces*

As discussed in the introduction, local damage identification using substructure separation methods is usually performed by partitioning the equation of motion of the global structure and separating the equation of motion of the substructure, which requires a parametric numerical model of the substructure and a corresponding parametrization of the damage. As a result, the separated substructure is coupled to the global structure via the generalized interface forces, which need to be estimated or identified along with the damage. This section uses a custom substructure separation method; the damage and the interface forces are identified using an optimization procedure similar to that described in [21]. Other approaches to the inverse problem of simultaneous identification of loads and damages are discussed e.g. in [22, 23].

The separated substructure with free boundary is shown in Figure 7; it is coupled to the global structure via the interface forces f_2 and f_3. Let the substructure be divided into five segments, as shown in Figure 8. The damage is modeled by decreasing the stiffnesses of the segments, and it is represented by the vector of the stiffness reduction ratios $\boldsymbol{\mu} = \{\mu_1, \mu_2, \ldots, \mu_5\}$, where $\mu_i \in (0, 1]$ is

Prepared using stcauth.cls

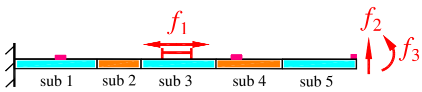

Figure 8. Division of the substructure into segments (sub-parts) for the purpose of damage identification

the ratio of the decreased stiffness $\hat{K}_i$ of the ith segment to its original stiffness K_i,

$$\mu_i = \frac{\hat{K}_i}{K_i}. \tag{24}$$

In the experiment, only the second segment is actually damaged, and the actual damage is represented by

$$\boldsymbol{\mu}_{\text{actual}} = [1.00, 0.42, 1.00, 1.00, 1.00]^{\mathrm{T}}. \tag{25}$$

According to the separation approach, the aim is to identify the unknowns, which are the vector of the damage extents $\boldsymbol{\mu}$ and the interface forces f_2 and f_3, given the excitation f_1 (Figure 5) and the measured responses of the two inner (Y_1, Y_2) and two boundary sensors (Y_3, Y_4). This is accomplished here by minimization of the following objective function:

$$F(\boldsymbol{\mu}) = \sum_{i=1}^{4} \frac{\int_0^T \left\| \mathrm{Y}_i(\boldsymbol{\mu}, t) - \mathrm{Y}_i^{\mathrm{M}}(t) \right\|^2 dt}{\int_0^T \|\mathrm{Y}_i^{\mathrm{M}}(t)\|^2 \, dt}, \tag{26}$$

which is the normalized least-square distance between the measured responses and the computed responses. In Eq. (26), the vector $\mathbf{Y}^{\mathrm{M}}(t)$ collects the measured responses of the four sensors, while $\mathbf{Y}(\boldsymbol{\mu}, t)$ is the vector of the corresponding responses computed for the damage extents $\boldsymbol{\mu}$. The substructure is assumed to be linear, hence, given $\boldsymbol{\mu}$, these responses can be computed as

$$\mathrm{Y}_i(\boldsymbol{\mu}, t) = \int_0^T h_{i1}(\boldsymbol{\mu}, t) f_1(t) \, dt + \sum_{j=2}^{3} \int_0^T h_{ij}(\boldsymbol{\mu}, t) f_j(\boldsymbol{\mu}, t) \, dt, \tag{27}$$

where $h_{ij}(\boldsymbol{\mu}, t)$ are the corresponding impulse-response functions of the damaged substructure (with the damage defined by $\boldsymbol{\mu}$) and the interface forces $f_2(\boldsymbol{\mu}, t)$, $f_3(\boldsymbol{\mu}, t)$ are computed by solving in the least-squares sense the following linear deconvolution problem:

$$\mathrm{Y}_i^{\mathrm{M}}(t) - \int_0^T h_{i1}(\boldsymbol{\mu}, t) f_1(t) \, dt = \sum_{j=2}^{3} \int_0^T h_{ij}(\boldsymbol{\mu}, t) f_j(\boldsymbol{\mu}, t) \, dt. \tag{28}$$

The objective function Eq. (26) is used for separate identification of local damages in all three global structures that have been tested (Table II). The results are shown in Figure 9; they are reasonably accurate. The interface forces computed in the final step of each optimization are plotted in Figure 10. A clear disadvantage of the separation approach is that the interface forces have to be reconstructed at each step of the optimization. This is done each time by solving a discretized version of Eq. (28), which is a time-consuming process: 4000 time steps are used, and Eq. (28) corresponds to an 8000×8000 discrete dense linear system. Moreover, if the placement of the excitation f_1 is unknown, the identification using this method is hard to be performed.

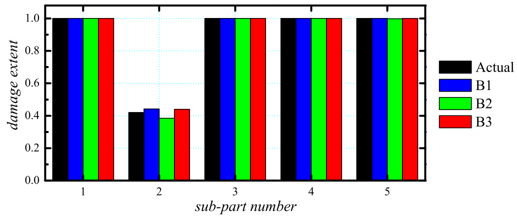

Figure 9. Actual damage and the damage identified in beams B1, B2 and B3 (Table II) using a substructure separation approach

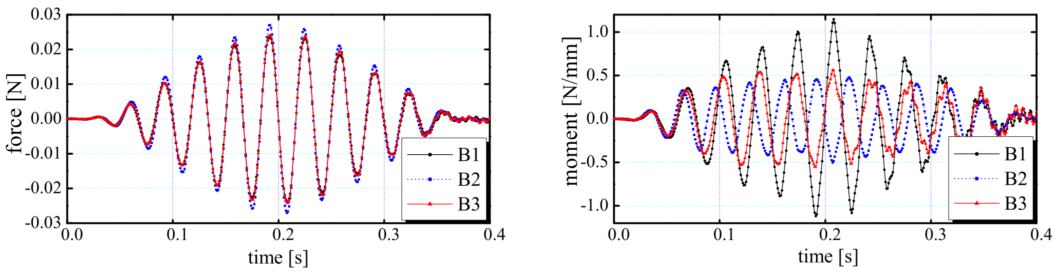

Figure 10. Identified interface forces in beams B1, B2 and B3: (*left*) f_2; (*right*) f_3

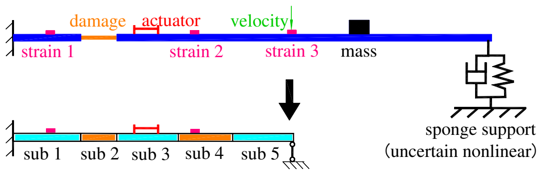

Figure 11. Isolation of the substructure with a single virtual pinned support in the interface node (free support in the rotational DOF, fixed support in the transverse DOF, negligible axial distortions)

5.3. Isolation with virtual supports

In order to avoid repeated identification of the interface forces, the substructure isolation method is used to identify the damage. A single virtual pinned support is used to isolate the substructure in the interface node, see Figure 11. As axial distortions are negligible, it is implemented by the two interface sensors: the strain sensor "strain 3" plays the role of the free support in the rotational DOF and constrains the bending moment, while the velocity sensor plays the role of the fixed support and constrains the transverse displacement. The two other strain sensors ("strain 1" and "strain 2") are placed in the inner substructure and used for damage identification. As two virtual supports are used, two constraining excitations are required. They are applied at two points of the outside structure; the locations are denoted by P2 and P3 (Table III). There is no limitation on the type of the constraining excitation, so a common uninstrumented hammer is used to apply simple transverse impacts. In order to ensure that the corresponding responses are independent, P2 and P3 are far from each other.

Table III. Excitations

symbol	excitor	position
P1	piezo-actuator/hammer	inner substructure
P2	hammer	upper outside structure
P3	hammer	lower outside structure

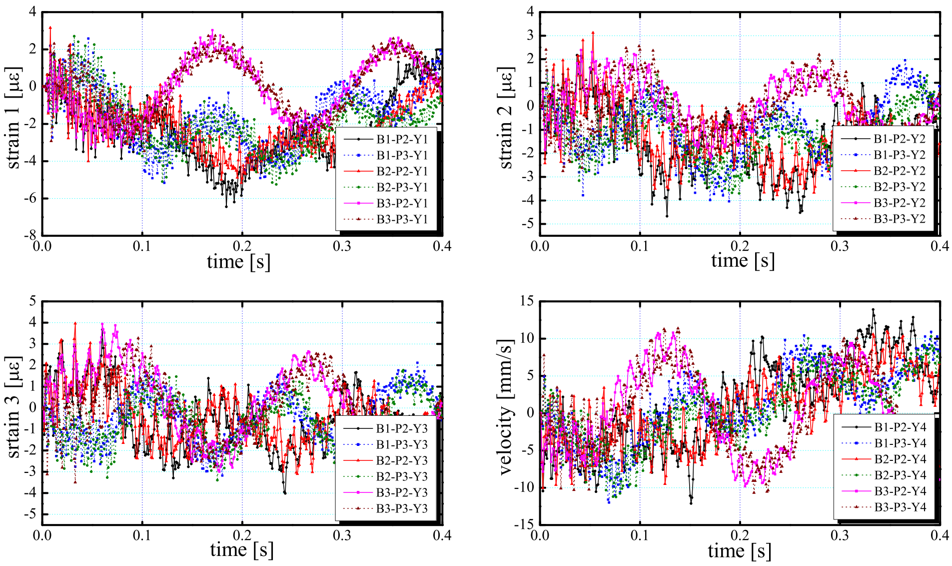

Figure 12. Measured constraining responses of the three considered global structures: (*upper left*) strain Y1; (*upper right*) strain Y2; (*bottom left*) strain Y3; (*bottom right*) velocity Y4

5.3.1. Identification in time domain If the basic excitation, which is applied inside the substructure, is known, local damages can be identified in time domain using the constructed responses of the isolated substructure. The basic response is excited by f_1 at the location P1, see Figure 5 and Figure 6. The constraining responses of the four sensors in the three global structures are shown in Figure 12. Notice that they are significantly different in the structures B1, B2 and B3 (Table II).

The substructure is isolated by Eq. (20), which involves the basic and the constraining responses. These can be measured in any of the three global structures B1, B2 or B3. Figure 13 plots the three corresponding responses of the isolated substructure. The responses are visually undistinguishable; it is consistent with the fact that all three global structures have the same substructure. The influences of the outside structures, including the additional mass and the sponge support, are eliminated.

Each of the responses in Figure 13 is constructed using the measurements of the same global structure, out of three possible. In order to verify the robustness of the method in case of a changing global structure, the basic and the constraining responses can be measured in different global structures. As there are three global structures, there are nine combinations, which are denoted by "bX-cY" (e.g. "b1-c2" stands for the response constructed using the basic response (b) of B1 and the constraining response (c) of B2). Figure 14 plots all the nine responses constructed this way along with the responses

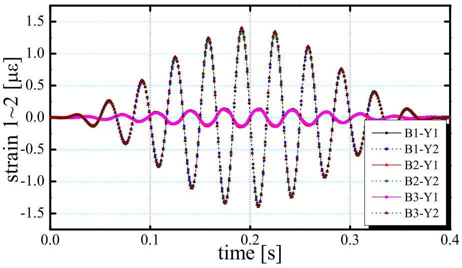

Figure 13. Constructed responses Y1 and Y2 of the same substructure isolated out of the three considered global structures (B1, B2 and B3, see Table II)

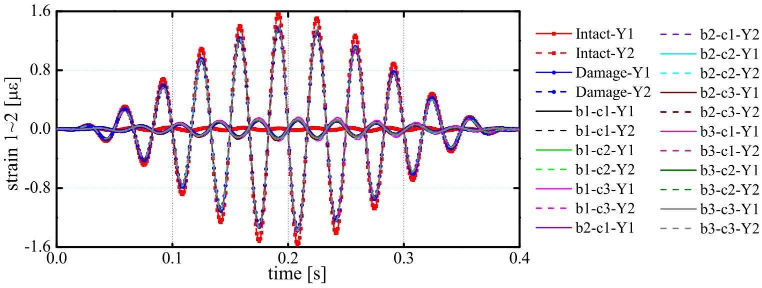

Figure 14. Responses of the isolated substructure: the nine constructed responses and the responses computed using FE models. The constructed responses are denoted by "bX-cY", which stands for the basic and the constraining responses measured respectively in the global structures BX and BY (Table II)

computed using FE models of the intact and the damaged substructures. The constructed responses match very well to each other and to the responses computed using the FE model of the damaged substructure. It confirms that the constructed response is not influenced by even developing unknown modifications of the outside structure, provided the substructure remains the same.

Damage identification in time domain amounts to the minimization of the objective function Eq. (22). First, assume that the location of the damage is known, so that only μ_2 should be identified. Figure 15 plots the nine objective functions, which correspond to the nine constructed responses of the substructure. All the minima are not far from the actual value of 0.42. Next, all five ratios μ_1 to μ_5 are assumed to be unknown. The identification results are shown in Figure 16 and compared to the actual values. Both the location and the extent of the damage are identified accurately, even though the outside structures were different or changing.

5.3.2. Identification in mode domain Sometimes the basic excitation can be hard to be properly designed or measured. In real applications, hammer impact is the most practical excitation, so it can be used as the basic excitation instead of the actuator. The local damage can be then identified in mode domain using the modes of the isolated substructure.

In this experiment, two kinds of global structure (B1 and B3) are considered, and the Amplified Piezo Actuator (APA) is removed. Simple hammer impacts are applied respectively at the positions P1, P2 and P3 of beams B1 and B3 in order to obtain the corresponding basic (P1) and constraining (P2, P3) responses. As there are two global structures, there are four combinations of the basic/constraining

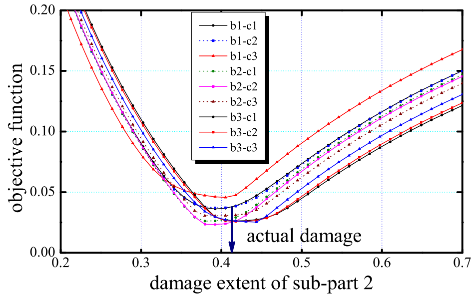

Figure 15. Objective functions corresponding to the nine constructed responses of the isolated substructure. Only the damage of the second segment (μ_2) is assumed to be unknown

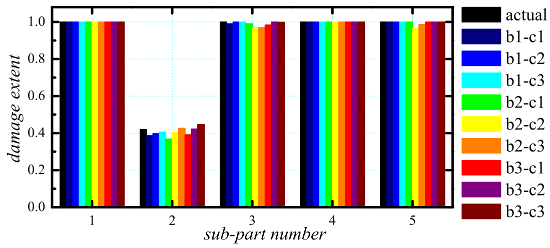

Figure 16. Actual damage and the results of damage identification in time domain; "bX-cY" denotes the result obtained with the basic and the constraining responses measured respectively in the global structures BX and BY (Table II)

responses that can be used to construct four responses of the isolated substructure.

Hammer impacts last for a very short time. The constructed response after the impact is free response, which can be used to identify the natural frequencies of the isolated substructure by the Eigensystem Realization Algorithm (ERA). Normally, mode shapes are also used for identification, see Eq. (23). Here, the number of the sensors located in the inner of the substructure is not enough to estimate the error of mode shapes by MAC, so only the natural frequencies are used to identify the substructure. In this way, the voltage signal of sensors need not be calibrated. The four constructed voltage signals (without calibration) of the isolated substructure (Figure 11, without APA) can be seen in Figure 17. The first seven identified natural frequencies of the isolated substructure are shown in Table IV, which compares them with the natural frequencies obtained from the numerical models of the intact and damaged substructures. The damage is locally identified by minimizing the objective function Eq. (23), in which only the natural frequencies are used. The results identified with the four combinations of the basic/constraining responses are shown in Figure 18 and compared with the actual values. Both the damage locations and the extents are identified with an acceptable accuracy.

5.4. Discussion

In this section, three substructuring methods for local damage identification have been experimentally studied: Substructure Separation and Identification in Time Domain (SS&ITD), Substructure Isolation and Identification in Time Domain (SI&ITD), Substructure Isolation and Identification in Mode Domain (SI&IMD). They can be compared with regard to the following four aspects:

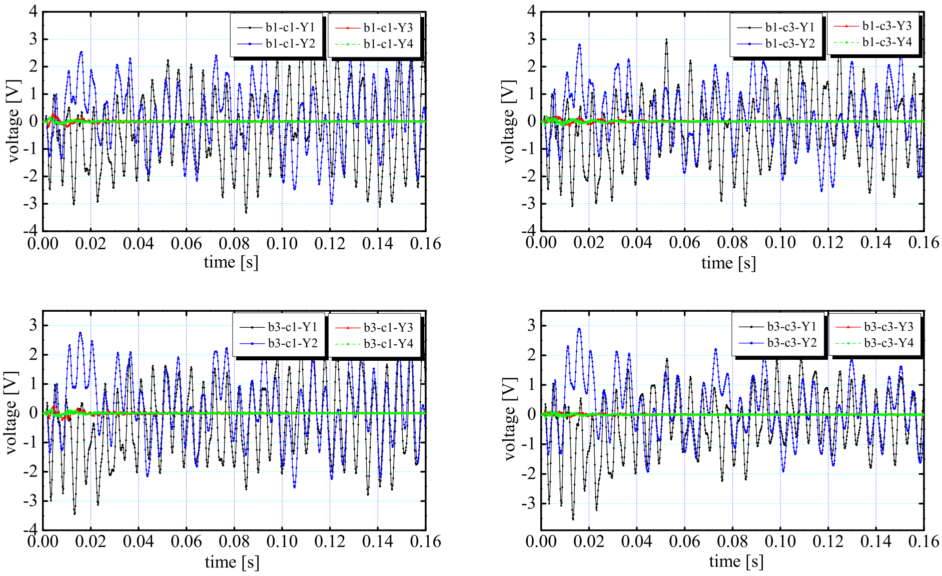

Figure 17. Constructed responses of the isolated substructure to an impact basic excitation (without calibration)

Table IV. Identified natural frequencies of the isolated substructure

Order	Intact	Damaged	b1-c1	b1-c3	b3-c1	b3-c3
1	17.69	17.52	16.93	16.70	16.97	16.99
2	57.33	52.01	51.73	51.77	52.29	52.31
3	119.15	112.95	112.59	112.85	112.00	111.91
4	203.30	195.66	195.40	195.52	193.33	193.35
5	310.47	290.04	287.58	288.24	289.85	289.89
6	439.95	413.93	415.34	415.34	415.03	414.93
7	592.48	551.07	551.42	551.27	550.82	550.87

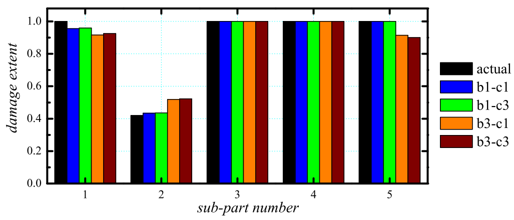

Figure 18. Actual damage and the results of damage identification in mode domain; "bX-cY" denotes the result obtained with the basic and the constraining responses measured respectively in the global structures BX and BY (Table II)

- *Efficiency.* Isolation seems to be more efficient than Separation. In the separation method, the interface forces have to be computed in each iteration during the optimization, which is time-consuming. In the isolation approach, the isolation is performed only once, before the identification process.
- *Flexibility.* Isolation seems to be more flexible than Separation. After isolation of substructure, the damage can be identified in time domain, in mode domain or using any other of the standard and well-researched damage assessment methods that were originally aimed at global analysis. In the separation approach, the damage has to be identified together with the interface forces, so that any damage identification method has to be non-standard and specifically tailored to be used on the substructural level.
- *Accuracy.* The identification in time domain has higher accuracy than that in mode domain. The response in time domain contains more information about the dynamics of the substructure, while the modal truncation error is unavoidable in mode-based identification. Therefore, the damage extents identified by both SS&ITD and SI&ITD are more precise than that identified by SI&IMD.
- *Limitations.* The limitation of substructure isolation method is that the responses of all interface DOFs should be measured for isolation.

6. CONCLUSIONS

This paper discussed, extended and experimentally studied the substructure isolation method. The method can be applied for local structural health monitoring and damage identification, as it virtually isolates the substructure from a large and complex global structure into a simple, small and independent structure. Both the theoretical deductions and the experimental verification confirm that a substructure can be effectively isolated by placing virtual fixed or free supports in its interface degrees of freedom (DOFs), so that its inner sensors respond to local excitations only. As a result, local-only information is extracted from the measured response of the global structure. It can be then used for local identification using a variety of existing, well-investigated methods that have been originally aimed at global analysis in time domain, mode domain or others. The instrumentation and computational costs of such a local analysis can be significantly reduced in comparison to the costs of a global analysis of the entire structure.

The method is flexible and easily implementable in practice. The influences of the outside structure are eliminated from the measured responses of the substructure using experimental data only, so that no numerical modeling is necessary for isolation. In contrast to many other substructuring methods, the interface forces need not be identified, which decreases the computational costs. Only the interface DOFs need to be all instrumented, while the number of the inner sensors depends solely on the method used for local analysis; far fewer inner sensors can be thus required. Moreover, the outside structure is completely irrelevant to the isolation process, so that it can be linear or nonlinear, continually changing or simply unknown. In the experiment, the substructure could be successfully isolated and identified even though the outside structures were different or changing.

The necessity to measure the responses in all DOFs of the substructure interface remains a limitation of the discussed substructure isolation method. In case of a hardly accessible boundary, it restricts the applicability of the method. This limitation is a subject of an ongoing research.

Prepared using stcauth.cls

ACKNOWLEDGEMENTS

The authors gratefully acknowledge the support of the Key Project of Natural Science Foundation of China #50538020 and of the Project of National Key Technology R&D Program (China) #2006BAJ03B05. Financial support of Structural Funds in the Operational Programme - Innovative Economy (IE OP) financed from the European Regional Development Fund - Projects "Modern material technologies in aerospace industry" (NoPOIG.0101.02-00-015/08) and "Health monitoring and lifetime assessment of structures" (POIG.0101.02-00-013/08-00) is gratefully acknowledged.

REFERENCES

1. Park KC, Reich GW, Alvin KF. Structural Damage Detection Using Localized Flexibilities. *Journal of Intelligent Material Systems and Structures* 1998; **9**(11):911–919.
2. Park KC, Reich GW. Use of substructural transmission zeros for structural health monitoring. *AIAA Journal* 2000; **38**(6):1040–1046.
3. Bernal D. Load Vectors for Damage Localization. *Journal of Engineering Mechanics* 2002; **128**(1):7–14.
4. Bernal D, Gunes B. Flexibility Based Approach for Damage Characterization: Benchmark Application *Journal of Engineering Mechanics* 2004; **130**(1):61–70.
5. Gao Y, Spencer B. Damage localization under ambient vibration using changes in flexibility *Earthquake Engineering and Engineering Vibration* 2002; **1**(1):136–144.
6. Koh CG, See LM, Balendra T. Estimation of structural parameters in time domain: a substructure approach. *Earthquake Engineering and Structural Dynamics* 1991; **20**(8):787–801.
7. Koh CG, Hong B, Liaw CY. Substructural and progressive structural identification methods . *Engineering Structures* 2003; **25**(12):1551–1563.
8. Oreta AWC, Tanabe T. Element Identification of Member Properties of Framed Structures. *Journal of Structural Engineering* 1994; **120**(7):1961–1976.
9. Yun C-B, Lee H-J. Substructural identification for damage estimation of structures. *Structural Safety* 1997; **19**(1):121–140.
10. Tee KF, Koh CG, Quek ST. Substructural first- and second-order model identification for structural damage assessment. *Earthquake Engineering and Structural Dynamics* 2005; **34**(15):1755–1775.
11. Tee KF, Koh CG, Quek ST. Numerical and experimental studies of a substructural identification strategy. *Structural HEalth Monitoring* 2009; **8**(5):397–410.
12. Koh C, Shankar K. Substructural identification method without interface measurement. *Journal of Engineering Mechanics (ASCE)* 2003; **129**(7):769–776.
13. Yang JN, Huang HW. Substructure damage identification using sequential nonlinear LSE method. In *4th International Conference on Earthquake Engineering* October 12–13, 2006: Taipei, Taiwan.
14. Yun C-B, Bahng EY. Substructural identification using neural networks. *Computers and structures* 2000; **77**(1):41–52.
15. Hou J, Jankowski Ł, Ou J. A substructure isolation method for local structural health monitoring. *Structural Control & Health Monitoring*; in press.
16. Holnicki-Szulc J, Gierliński J. *Structural Analysis, Design and Control by the Virtual Distortion Method.* John Wiley & Sons Ltd, Chichester, 1995.
17. Kołakowski P, Wikło M, Holnicki-Szulc J. The virtual distortion method—a versatile reanalysis tool for structures and systems. *Structural and Multidisciplinary Optimization* 2008; **36**(3):217–234.
18. Holnicki-Szulc J. (ed.) *Smart Technologies for Safety Engineering.* John Wiley & Sons Ltd, Chichester, 2008.
19. Kress R. *Linear integral equations.* Springer, New York, 1989.
20. Hansen PC. Deconvolution and regularization with Toeplitz matrices. *Numerical Algorithms* 2002; **29**(4): 323–378.
21. Zhang Q, Jankowski Ł, Duan Z. *Fast identification of loads and damages using a limited number of sensors.* 5th European Workshop on Structural Health Monitoring, 29 June – 02 July 2010, Sorrento, Italy.
22. Lu Z, Law S. Identification of system parameters and input force from output only. *Mechanical Systems and Signal Processing* 2007; **21**(5): 2099–2111.
23. Zhang Q, Jankowski Ł, Duan Z. Identification of coexistent load and damage. *Structural and Multidisciplinary Optimization* 2009; in press. doi 10.1007/s00158-009-0421-1.
24. Juang J-N, Pappa RS. An eigensystem realization algorithm for modal parameter identification and model reduction. *Journal of Guidance, Control, and Dynamics* 1985; **8**(5): 620–627.